

EURAD-IM

Products, Quality and Background Information

Contributors :

Hendrik Elbern, Elmar Friese (FRIUUK, #21)

Editors :

Hendrik Elbern, R-EDA leader (FRIUUK, #21)

Vincent-Henri Peuch, R-ENS leader (METEO-FR, #15)

Laurence Rouil, R-EVA leader (INERIS, #23)

Contact :

he@eurad.uni-koeln.de



EURAD-IM facts sheet

1. Products portfolio

Name	Description	Freq.	Available	Species	Time span
FRC	Forecast at the surface, 500m, 1000m, 3000m, and 5000m above ground	Daily	4 UTC	O ₃ , NO, NO ₂ , CO, SO ₂ , PM _{2.5} , PM ₁₀	0-72h, hourly
ANA	Analysis at the surface	Daily, hourly assimilation	2 UTC for the day before	O ₃ , NO, NO ₂ , CO, SO ₂ , PM _{2.5} , PM ₁₀	0-24h, hourly

2. Performance statistics

See annexes.

3. Availability statistics

Quarter 8 (March, April, May 2011): 96% and 93% of the EURAD-IM forecasts and analyses have been provided in time.

Forecasts were missing or strongly delayed on 12, 17, 31 March and 7 April. Analyses were missing or strongly delayed on 7, 15, 16, 24 March, 11 April and 8 May. Delayed forecasts and analyses were related to temporal unavailability of compute nodes or the data storage system, or delayed input data (observations).

Quarter 9 (June, July, August 2011): 96% and 98% of the EURAD-IM forecasts and analyses have been provided in time.

Delayed forecasts and analyses were related to temporal unavailability of compute nodes or the data storage system, or delayed input data (observations).

4. Assimilation and forecast system: synthesis of main characteristics

Assimilation and Forecast System	
Horizontal resolution	15 km on a Lambert conformal projection
Vertical resolution	23 layers up to 100 hPa Lowest layer thickness about 35 m About 15 layers below 2 km
Gas phase chemistry	RACM-MIM
Heterogeneous chemistry	N ₂ O ₅ hydrolysis: RH dependent parameterization
Aerosol size distribution	Three log-normal modes: two fine + one

	coarse, fixed standard deviation
Inorganic aerosols	Thermodynamic equilibrium for the H^+ - NH_4^+ - SO_4^{2-} - NO_3^- - H_2O system
Secondary organic aerosols	SORGAM module
Aqueous phase chemistry	10 gas/aqueous phase equilibria 5 irreversible S(IV) \rightarrow S(VI) transformations
Dry deposition/sedimentation	Resistance approach/size dependent sedimentation velocity
Mineral dust	DREAM model
Sea Salt	Included
Boundary values	MOZART IFS forecast for the day before
Initial values	3d-var analysis for the day before
Anthropogenic emissions	TNO (2005) inventory with $0.125^\circ \times 0.0625^\circ$ resolution
Biogenic emissions	NKUA monthly biogenic emission potentials
Forecast System	
Meteorological driver	MM5V3 forced by 12:00 UTC operational IFS forecast for the previous day
Assimilation System	
Assimilation method	Intermittent 3d-var
Observations	Surface in situ data from France, Germany, and the EEA, Atmospheric NO_2 column retrievals from AURA/OMI, METOP/GOME-2, and ENVISAT/SCIAMACHY
Frequency of assimilation	hourly
Meteorological driver	MM5V3 forced by 00:00 UTC operational IFS forecast

Evolutions in the EURAD-IM suite

2010/09/06: improved calculation of photolysis frequencies in cloudy conditions.

2010/04/21: improved temporal variation of emission rates, modified VOC split.

2010/03/12: application of TNO MACC emission inventory with base year 2005.

2010/01/08: implementation of an AOD observation operator.

2009/08/26: improved meteorological auxiliary parameter calculation (horizontal wind at 10m) for sea salt modelling.

2009/06/01: start of MACC pre-operational forecasts.

2009/06/01: start of daily MACC 3d-var analysis.

EURAD-IM background information

1. Forward model

The EURAD model system consists of 5 major parts: the meteorological driver MM5 (version 3), the pre-processors EPC and PREP for preparation of meteorological fields and observation data, respectively, the EURAD Emission Model EEM (Memmesheimer, 1991) and the chemistry transport model EURAD-IM. The data flow of the EURAD system is depicted in Figure 1 (Hass, 1991, Ackermann et al., 1998, Memmesheimer et al., 2004). EURAD-IM is a mesoscale chemistry transport model involving transport, diffusion, chemical transformation, wet and dry deposition and sedimentation of tropospheric trace gases and aerosols.

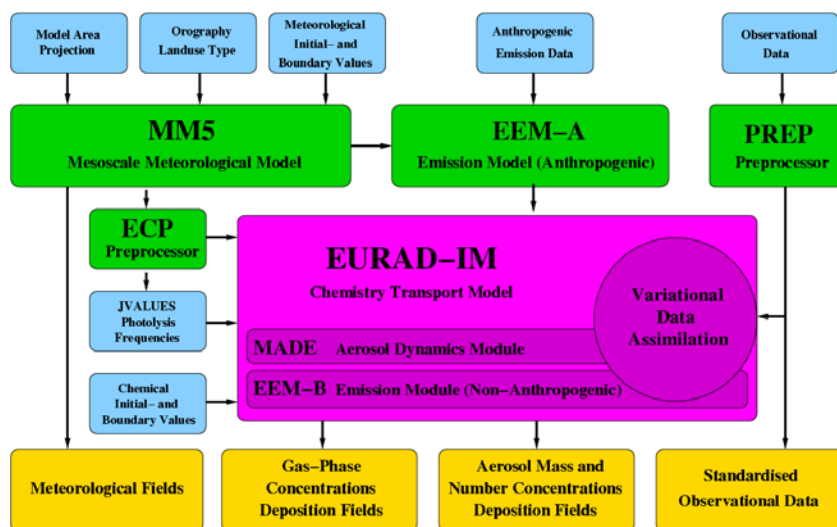


Figure 1: Flowchart of the EURAD-IM model system containing the meteorological driver MM5, the pre-processors ECP and PREP, the emission model EEM and the chemistry transport model EURAD-IM (input parameters are shaded in blue, output parameters are shaded in yellow and procedural parts are shaded in green or magenta).

EURAD-IM includes 4d-var chemical data assimilation (Elbern et al., 2007) and is able to run in nesting mode.

1.1 Model geometry

To cover the MACC domain from 15°E to 35°W and 35°N to 70°N a Lambert conformal projection with 15 km horizontal resolution (317x287 grid boxes) is used. In the vertical the atmosphere is divided by 23 terrain-following sigma coordinate layers up to 100 hPa. About 15 layers are below 2 km height. The thickness of the lowest layer is about 35 m.

1.2 Forcing and boundary values

MM5V3 forced by the operational IFS forecast is used to provide the meteorological fields which are needed to run the EURAD-IM CTM. Hourly MM5 output is linearly interpolated in time within the CTM on the current model time.

Chemical boundary values of gas phase constituents are derived from the operational MOZART IFS forecast for the day before. Three hourly MOZART IFS output of concentration fields of 20 species are area weighted horizontally interpolated, linearly interpolated in the vertical and in time, and assigned to the appropriate chemical species within the EURAD-IM CTM.

Chemical initial values are provided by a 3d-var analysis for the previous day.

1.3 Dynamical core

To propagate a set of chemical constituents forward in time the EURAD-IM CTM solves a system of partial differential equations:

$$\frac{\partial c_i}{\partial t} = -\nabla(\vec{v} c_i) + \nabla(\rho \mathbf{K} \nabla \frac{c_i}{\rho}) + A_i + E_i - S_i,$$

where c_i is the mean mass mixing ratio of chemical species i , \mathbf{v} are mean wind velocities, \mathbf{K} is the eddy diffusivity tensor, ρ is air density, A_i is the chemical generation term for species i , E_i and S_i its emission and removal fluxes, respectively. The numerical solution of the above equation has its difficulties due to the different numerical characters of the major processes. To overcome these problems an operator splitting technique is employed (McRae, 1982), wherein each process is independently treated in a sequence. The EURAD-IM CTM uses a symmetric splitting of the dynamical processes, encompassing the chemistry solver **C**:

$$c_i^{t+\Delta t} = T_h T_v D_v C D_v T_v T_h c_i^t,$$

where $T_{h,v}$ and D_v denote transport and diffusion operators in horizontal (h) and vertical (v) direction. The emission term is included in **C**.

The CTM's basic time-step Δt depends on the horizontal and vertical grid resolution in order to fulfill the CFL-criterion. If this criterion is locally not fulfilled, the time-step is dynamically adapted. $\Delta t_T = \Delta t/2$ is the transport time step used for the advection and diffusion with operators $T_{h,v}$ and D_v . For the gas phase chemistry calculations the basic time step Δt is split into a set of variable time steps, which are often considerably smaller than Δt according to the chemical situation.

The positive definite advection scheme of Bott (1989), implemented in a one-dimensional realization, is used to solve the advective transport. An Eddy diffusion approach is used to parameterize the vertical sub-grid-scale turbulent transport. The calculation of vertical Eddy diffusion coefficients is based on the specific turbulent structure in the individual regimes of the planetary boundary layer (PBL) according to the PBL height and the Monin-Obukhov length (Holtslag and Nieuwstadt, 1986). A semi-implicit (Crank-Nicholson) scheme is used to

solve the diffusion equation. Dry deposition is applied as lower boundary condition of the diffusion equation.

1.4 Physical Parameterizations

1.4.1 Photolysis frequencies

Photolysis frequencies are derived according to Madronich (1987). Actinic fluxes are calculated by a radiative transfer model based on the delta-Eddington technique for a grid of 130 spectral intervals from 1 to 10 nm. The height from the surface of the earth to the top of the atmosphere is divided into 50 layers. Products of the absorption cross section, the quantum yield, and the actinic flux are integrated over the spectral range to produce a table of clear sky photolysis rates. For cloudy conditions, photolysis rates within the cloud layers are multiplied by a correction factor depending on the cloud fractional coverage and the cloud optical thickness.

1.4.2 Aerosol dynamics

The aerosol dynamics model MADE (Ackermann et al., 1998) is used to provide information on the aerosol size distribution and chemical composition (see Figure 2). Fine particles smaller than about 2.5 micrometers are treated by two interacting log-normal modes. The coarse particles form a third mode. The two smaller modes interact with each other through coagulation. Each mode may grow through condensation of gaseous precursors. The aerosol species treated in the two fine particle modes are secondary inorganic aerosols, primary and elemental carbon, other unspecified material of anthropogenic origin, and anthropogenic and biogenic secondary organic species. The SORGAM module (Schell et al., 2001) simulates secondary organic aerosol formation including the production of low-volatility products and their subsequent gas/particle partitioning. The coarse particles consist of unspecified material of anthropogenic origin, sea salt (Monahan et al., 1986; Martensson, 2003), and mineral dust (Nickovic et al., 2001).

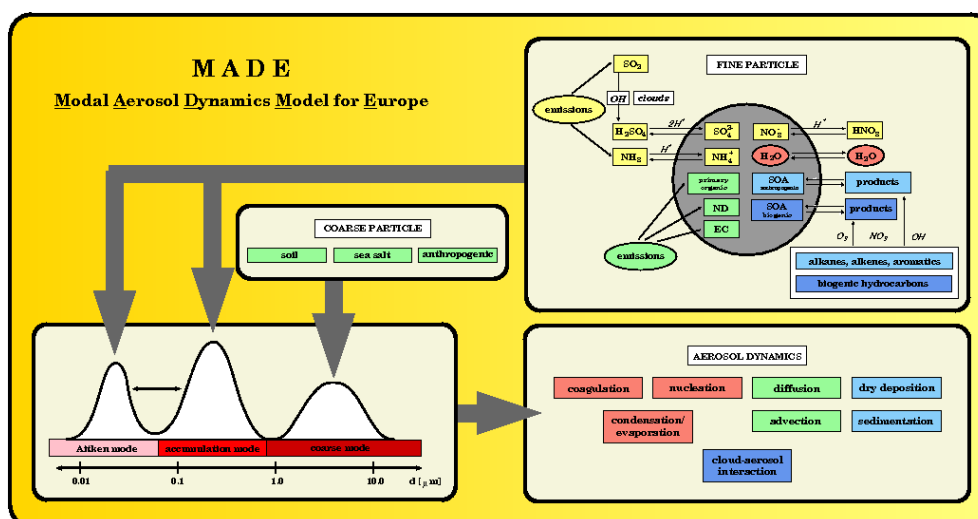


Figure 2: Schematic of the aerosol dynamics model MADE (see text for explanations).

1.4.3 Dry deposition and sedimentation

Dry deposition velocities of 20 gas phase species are calculated using a resistance model which considers the aerodynamic resistance, the quasi-laminar layer resistance, and ground and canopy resistances, respectively, depending on land use characteristics (Zhang et al., 2003).

The dry deposition and sedimentation of aerosol species is treated size dependent. For each of the three log-normal modes used within the EURAD-IM the dry deposition and sedimentation velocities are calculated using a resistance model (Ackermann et al., 1998).

1.4.4 Sub-grid convective clouds

The sub-grid cloud scheme in EURAD-IM was derived from the cloud model in the EPA Models-3 Community Multiscale Air Quality (CMAQ) modelling system (Roselle and Binkowski, 1999). Cloud effects on both gas phase species and aerosols are simulated by the cloud module. The effects of sub-grid clouds on grid-averaged concentrations are parameterized by modelling the mixing, scavenging, aqueous chemistry, and wet deposition of a 'representative cloud' within the grid cell. For all sub-grid clouds, a 1-hour live time has been assumed.

Pollutant scavenging is calculated by two methods, depending upon whether the pollutant participates in the cloud water chemistry and on the liquid water content. (1) For those pollutants that are absorbed into the cloud water and participate in the cloud chemistry, the amount of scavenging depends on Henry's law constants, dissociation constants, and cloud water pH. (2) For pollutants, which do not participate in aqueous chemistry, the model uses the Henry's law equilibrium to calculate ending concentration and deposition amount.

The accumulation mode and coarse mode aerosols are assumed to be completely absorbed by cloud water and rain water. The Aitken mode components are treated as interstitial aerosol and are slowly absorbed into the cloud/rain water.

1.5 Chemistry

1.5.1 Gas phase

The RACM-MIM chemical mechanism is used to treat the gas phase chemistry (Geiger et al., 2003). This mechanism includes 17 stable inorganic species, 4 inorganic intermediates, 36 stable organic species, and 27 organic intermediates. The mechanism includes 265 reactions. A two step Rosenbrock method is used to solve the set of chemical reactions (Sandu et al., 2003, Sandu and Sander, 2006).

1.5.2 Aqueous phase

Some rapidly established equilibria between the gas and aqueous phase (HNO_3 , N_2O_5 , NH_3 , O_3 , H_2O_2 , SO_2 , formic acid, methyl hydrogen peroxide, and peroxy acetic acid) are superimposed on 5 irreversible reactions (H_2O_2 , O_3 , methyl hydrogen peroxide, O_2

catalysed by iron and manganese, and peroxy acetic acid) involved in the conversion of S(IV) to S(VI) (Walcek and Taylor, 1986). All new sulphate produced in the aqueous-phase changes the aerosol accumulation mode mass (Binkowski, 1999).

1.5.3 Aerosol phase

Thermodynamic equilibrium is assumed for the system $\text{H}^+\text{-NH}_4^+\text{-SO}_4^{2-}\text{-NO}_3^-\text{-H}_2\text{O}$. To solve for the concentrations of these inorganic aerosol components a FEOM (fully equivalent operational model) version, using the HDMR (high dimensional model representation) technique (Rabitz et al., 1999, Nieradzik, 2005), of an accurate mole fraction based thermodynamic model (Friese and Ebel, 2010) is used.

2. Assimilation system

The three-dimensional variational data assimilation version of the EURAD-IM aims to minimize the following cost function:

$$J(\mathbf{x}) = \frac{1}{2} [\mathbf{x} - \mathbf{x}^b]^T \mathbf{B}^{-1} [\mathbf{x} - \mathbf{x}^b] + \frac{1}{2} [\mathbf{y} - H(\mathbf{x})]^T \mathbf{R}^{-1} [\mathbf{y} - H(\mathbf{x})]$$

with \mathbf{x} being the current model state with background knowledge \mathbf{x}^b , H the observation operator, \mathbf{B} the background error covariance matrix, \mathbf{R} the observation error covariance matrix and \mathbf{y} a set of observations. The minimum will be found by evaluating the gradient of the cost function with respect to the control variables \mathbf{x} ,

$$\nabla_{\mathbf{x}} J = \mathbf{B}^{-1} [\mathbf{x} - \mathbf{x}^b] + \mathbf{H}^T \mathbf{R}^{-1} [\mathbf{y} - H(\mathbf{x})]$$

with \mathbf{H}^T being the adjoint of the observation operator H . The quasi-Newton limited memory L-BFGS algorithm described in Nocedal (1980) and Liu and Nocedal (1989) is applied for the minimization. The assimilation procedure is taken as successfully finished after the minimum is attained.

The observation operator is needed to get the model equivalent to each type of measurement, yielding the possibility to compare the model state to various kinds of observations. A powerful observation operator is implemented in the current version of the EURAD-IM data assimilation system to get to assimilate heterogeneous sources of information like ground-based in situ measurements (currently used are measurements from Germany, France, and from the EEA) as well as retrieval products of satellite observations (currently used are atmospheric NO_2 column retrievals from AURA/OMI, METOP/GOME-2, and ENVISAT/SCIAMACHY), even using averaging kernel information.

Following Weaver and Courtier (2001) with the promise of a high flexibility in designing anisotropic and heterogeneous influence radii, a diffusion approach for providing \mathbf{B} is implemented. Weaver and Courtier show that the diffusion equation serves as a valid operator for square-root covariance operator modelling by suitable adjustments of local diffusion coefficients. For a detailed description of the properties of the implemented

background error covariance modelling as well as the observation error covariance matrix \mathbf{R} , see Strunk (2006) and Elbern et al. (2007).

3. Development plan

- Assimilation of MODIS aerosol optical depth measurements
- Implementation of a fire emission model including a plume rise module according to Freitas et al. (2007)

4. References

Ackermann, I.J., H. Hass, M. Memmesheimer, A. Ebel, F.S. Binkowski, and U. Shankar, *Atmos. Environ.*, **32**, 2981-2999, 1998.

Bott, A., *Mon. Wea. Rev.*, **117** (5), 1006-1015, 1989.

Binkowski, F.S., Aerosols in Models-3 CMAQ, in: *Science algorithms of the EPA Models-3 Community multiscale air quality (CMAQ) modeling system*, EPA 600/R-99-030, EPA, 1999.

Elbern, H., A. Strunk, H. Schmidt, and O. Talagrand, *Atmos. Chem. Phys.*, **7**, 1-59, 2007.

Freitas, S.R., K.M. Longo, R. Chatfield, D. Latham, M.A.F. Silva Dias, M.O. Andreae, E. Prins, J.C. Santos, R. Gielow, and J.A. Carvalho Jr., *Atmos. Chem. Phys.*, **7**, 3385-3398, 2007.

Friese, E. and A. Ebel, *J. Phys. Chem. A*, **114**, 11595-11631, 2010.

Geiger, H., I. Barnes, I. Bejan, T. Benter, and M. Spttler, *Atmos. Environ.*, **37**, 1503-1519, 2003.

Hass, H., *Description of the EURAD Chemistry-Transport-Model version 2 (CTM2)*, vol 83, *Mitteilungen aus dem Institut für Geophysik und Meteorologie der Universität zu Köln*, 1991.

Holtslag, A.A.M. and F.T.M. Nieuwstadt, *Boundary-Layer Met.*, **36**, 201-209, 1986.

Liu, D.C. and J. Nocedal, *Math. Programming*, **45**, 503-528, 1989.

Madronich, S., *J. Geophys. Res.*, **92**, 9740-9752, 1987.

Martensson, E.M., E.D. Nilsson, G. de Leeuw, L.H. Cohen, and H.-C. Hansson, *J. Geophys. Res.*, **108**, doi:10.1029/2002JD002263.

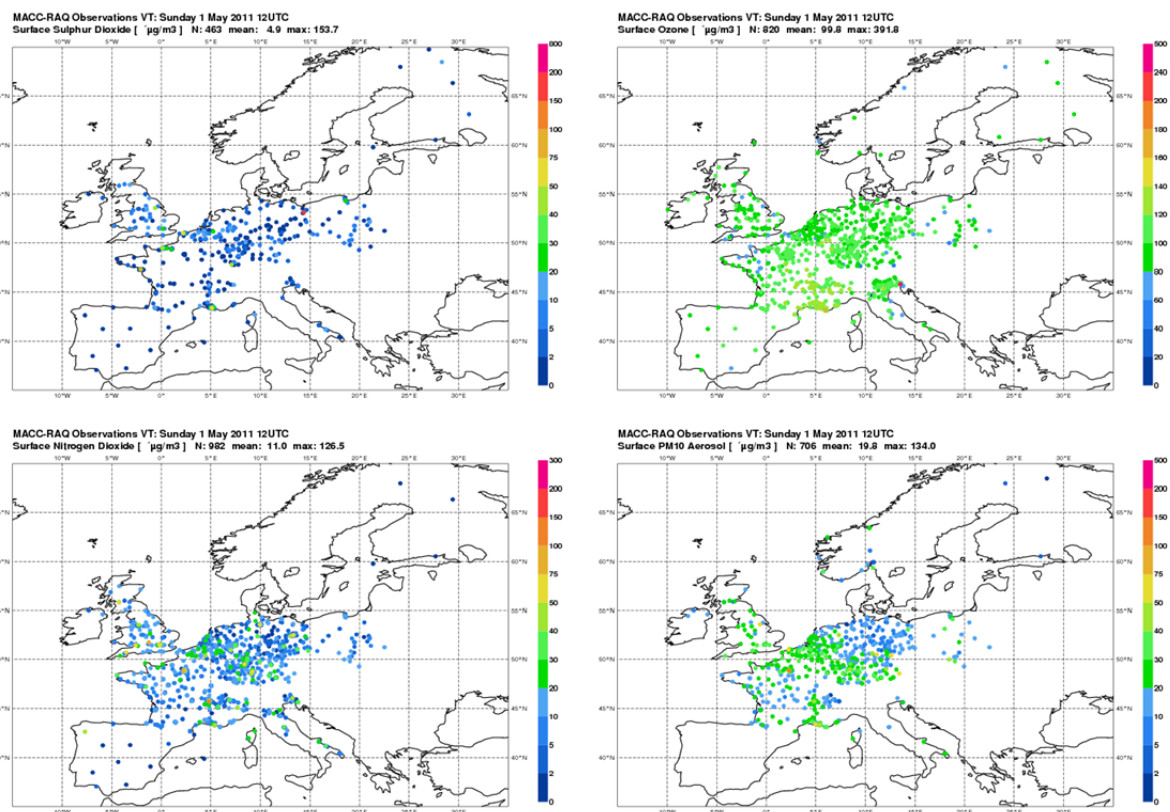
McRae, G.J., W.R. Goodin and J.H. Seinfeld, *J. Comp. Phys.*, **45**, 1-42, 1982.

- Memmesheimer, M., J. Tippke, A. Ebel, H. Hass, H.J. Jakobs, and M. Laube, On the use of EMEP emission inventories for European scale air pollution modelling with the EURAD model, in *Proceedings of the EMEP workshop on photooxidant modelling for long range transport in relation to abatement strategies*, edited by J. Pankrath, 307-324, UBA, Berlin, 1991.
- Memmesheimer, M., E. Friese, A. Ebel, H. J. Jakobs, H. Feldmann, C. Kessler and G. Piekorz, *Int. J. Environm. and Pollution*, **22**, (1-2), 108-132, 2004.
- Monahan, E.C., D.E. Spiel, and K.L. Davidson, in: *Oceanic Whitecaps*, E.C. Monahan and G. Mac Niocaill eds., 167-174, D. Reidel, Norwell, Mass., 1986.
- Nickovic, S., G. Kallos, A. Papadopoulos, and O. Kakaliagou, *J. Geophys. Res.*, **106**, 18113-18129, 2001.
- Nieradzik, L.P., *Application of a high dimensional model representation on the atmospheric aerosol module MADE of the EURAD-CTM*, Master Thesis, Institut für Geophysik und Meteorologie der Universität zu Köln, 2005.
- Nocedal, J., *Math. Comput.*, **35** (151), 773-782, 1980.
- Rabitz, H., O. Alis, J. Shorter, and K. Shim, *J. Math. Chem.*, **25**, 197-233, 1999.
- Roselle, S.J. and F.S. Binkowski, Cloud Dynamics and Chemistry, in: *Science algorithms of the EPA Models-3 Community multiscale air quality (CMAQ) modeling system*, EPA 600/R-99-030, EPA, 1999.
- Sandu, A., D. N. Daescu, and G.R. Carmichael, *Atmos. Environ.*, **37**, 5083-5096, 2003.
Sandu, A. and R. Sander, *Atmos. Chem. Phys.*, **6**, 187-195, 2006
- Schell, B., I.J. Ackermann, H. Hass, F.S. Binkowski, and A. Ebel, *J. Geophys. Res.*, **106**, 28275-28293, 2001.
- Strunk, A., *Tropospheric Chemical State Estimation by Four-Dimensional Variational Data Assimilation on Nested Grids*, Ph.D. Thesis, Institut für Geophysik und Meteorologie der Universität zu Köln, 2006.
- Walcek, C.J. and G.R. Taylor, *J. Atmos. Sci.*, **43**, 339-355, 1986.
- Weaver, A. and P. Courtier, *Q. J. R. Meteorol. Soc.*, **127**, 1815-1846, 2001.
- Zhang, L., J.R. Brook, and R. Vet, *Atmos. Chem. Phys.*, **3**, 2067-2082, 2003.

Verification report for quarter #8

This verification report covers the period March/April/May 2011. For this report, average skill scores (bias, root mean square error, correlation) for the EURAD-IM model are successively presented for three pollutants : ozone, NO₂ and PM10. The skill is shown for the entire forecast horizon 0 to 72h (3-hourly values), allowing to evaluate the entire diurnal cycle and the evolution of performance from day 1 to day 3.

For this verification period, as was the case on the MACC website, verifications are performed against all available data in Near-Real-Time (NRT) for the following countries: Belgium, Czech Republic, Denmark, Finland, France, Germany, Greece (Athens area only), Italy (not all regions), Netherlands, Norway, Poland, Spain, Sweden and the United Kingdom. The total number of sites is typically up to: 900 for ozone, 1200 for NO₂, 550 for SO₂, 300 for CO, 900 for PM10. As an example, the data coverage for Sunday May 1st 2011 12UTC is depicted below.

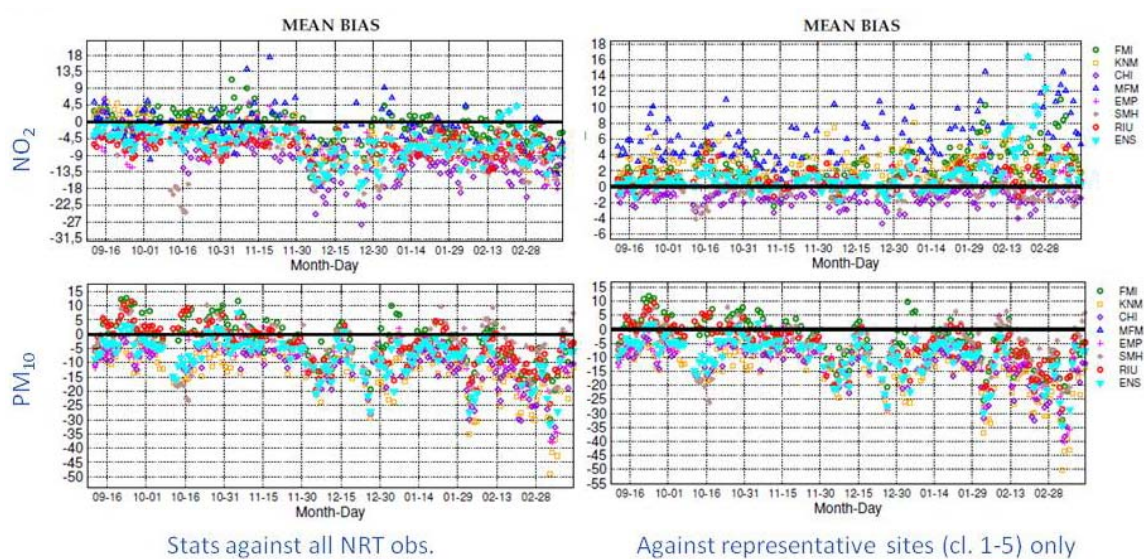


Near-Real-Time data coverage (May 1st 2011, 12 UTC)

Within MACC, the D-INSITU subproject is working with the European Environment Agency (EEA) to set up a new, more extensive and robust Near-Real-Time dataflow. An EEA European Air Quality data stream is available since the spring of 2011 and it has been checked by D-INSITU partners (in particular NILU) against the data currently received by MACC in NRT, which results from *ad hoc* bilateral agreement with Environment Agencies in

14 different countries. While there is an overlap between the two datasets, there is still a considerable number of differences. Briefly, the EEA dataset has more reporting sites for ozone and less for the other species. Also, there is a great interest in attempting to merge the two data sources, by helping for instance EEA to get access to data in the countries with which GEMS-MACC has been in contact and which do not provide all their NRT data to EEA. While this does not change the general objective to move to a EEA-based dataflow, it was felt that this evolution was not yet readily feasible for the last periods of MACC; this will be accomplished in MACC-II. A further advantage will be that data will arrive sooner, typically less than 3 hours after measurement. Currently, hourly data from the day before are available to MACC between 2 and 10 UT every day, depending on the country: this delays the possible start of daily verification calculations and makes it impossible to base the daily forecasts upon the analysis of the day before -as forecasts have to be delivered early enough every morning, in order to serve users' needs.

For the NRT verification of forecasts, the typology of sites is currently not taken into account: there is no uniform and reliable metadata currently for all regions and countries, which have all different approaches to this documentation. Skill scores are thus computed using all the data received. Within MACC, work has been carried out [Joly and Peuch, 2012] to build an objective classification of sites, based on the past measurements available in Airbase (EEA) ; see D_R-ENS_5.1 for more details. This classification can now be used in order to restrict verification only to the sites that have a sufficient spatial representativeness. Currently, about half of the sites used in the verification are declared "urban" in Airbase metadata and would be in principle not representative enough for comparing against forecast models that have horizontal resolutions of approximately 0.2°. However, our findings indicate that a significant fraction of sites labelled "urban" or "suburban" has actually little local character (as seen in past time series of measurements) and could be in fact more representative than what could be inferred from the metadata information. The figure below shows scores computed using all MACC data available in NRT and using only data for sites from classes 1-5 of our objective classification (the "background" fraction).



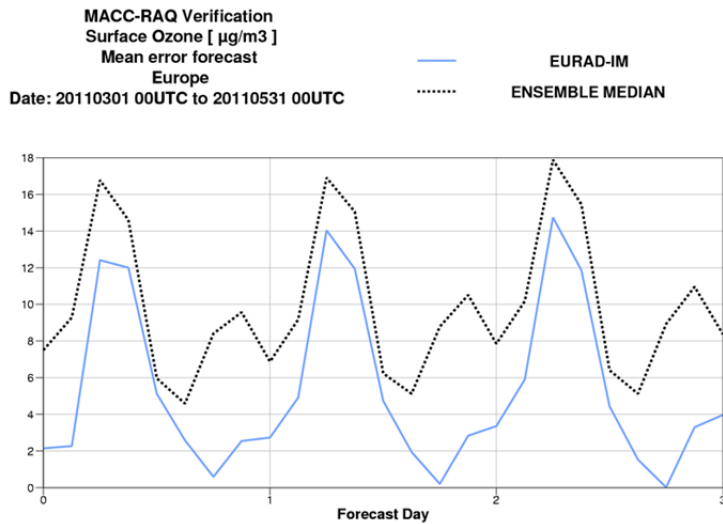
Sample model verification for the period 15/09/2010 to 28/02/2011 using all NRT sites (left) and using only most representative sites (classes 1-5) only (right). Values are for NO₂ (top) and PM₁₀ (bottom) for 0300 UTC.

While the statistical approach using only representative sites -according to the objective classification- is clearly the way forward (as it does not also thin too much the NRT data available), we see that overall skill scores are in general not too much affected by the observations from sites that have a local character, as illustrated here for PM10. Noticeable exceptions are winter night-time NO₂ values (top row on the figure), for which the general negative bias of the ensemble (around 5 µg.m⁻³) and of most of the individual models is entirely offset by using representative data only to compute skill scores.

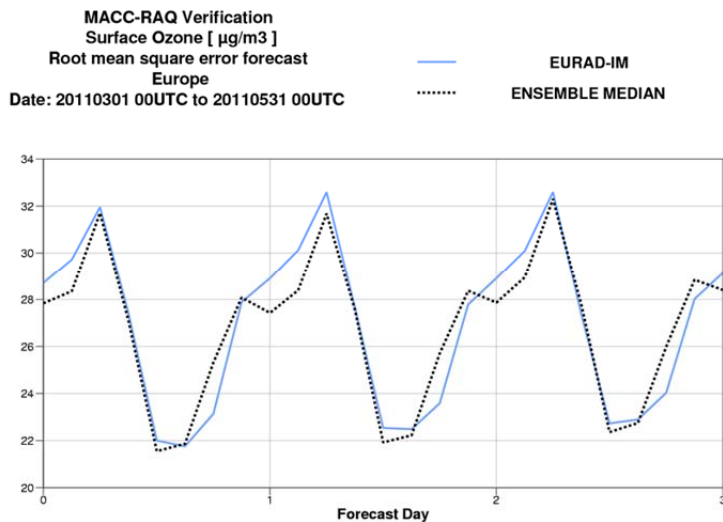
As this evolution does not induce dramatic changes to our assessment, we have opted to finalise MACC using “all NRT data” statistics (to have continuity of approach during the project) and to switch to the “representative sites only” statistics only from the first quarter of MACC-II (DJF 2011-2012). This approach will also contribute to alleviate the issue of the large variation in site densities from one country to another: the countries with higher densities of observational sites, particularly Germany and France, will actually “lose” many more sites than the others (also in proportion). Yet, the issue remains that the overall skill scores presented here, and also on the MACC website in NRT, are largely governed by the behaviour of the models in the “data intensive” countries. In MACC-II, our verification procedures will be more segmented (by countries and by large continental regions: Northern Europe, Eastern Europe, Mediterranean...), which will allow to be increasingly more specific on the description of AQ products quality. At the same time, we acknowledge that the amount of information provided has to remain within reasonable bounds, in order not to confuse general users.

Joly, M. and V.-H. Peuch, 2012: Objective Classification of air quality monitoring sites over Europe, Atmos. Env., 47, 111-123.

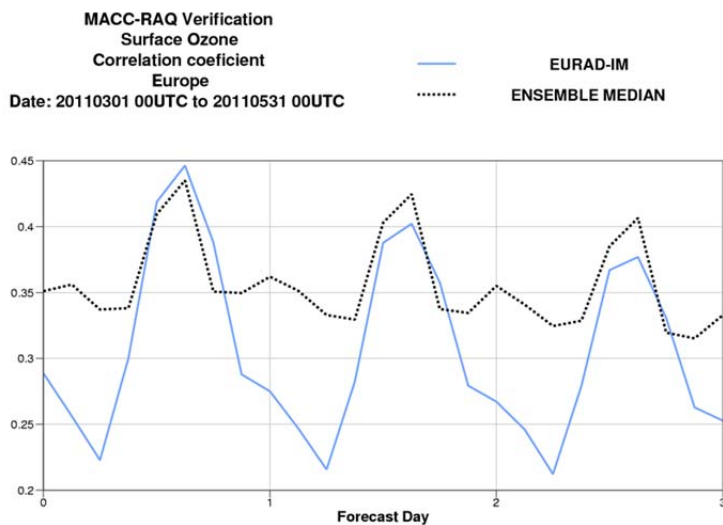
EURAD-IM: ozone skill scores, period #8 (March, April, May 2011)



The positive bias is largely due to the under estimation of Nitrogen Oxide at urban sites. Compared to the ensemble median the mean bias of surface Ozone is lesser. It is also lesser than for period #4 (March, April, May 2010) but a relative low bias during the first hours of the forecast, which would be an implication of the initialization of the forecast with the AQ analysis for the previous day, is no more visible.

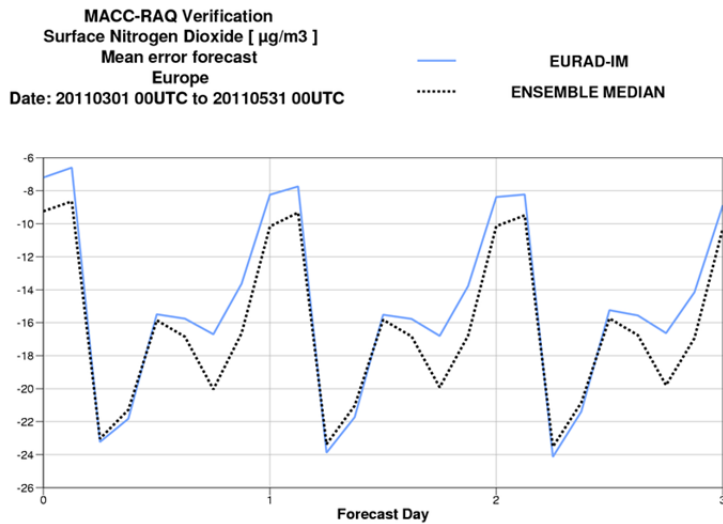


The root mean square error for surface Ozone is very similar to that of the ensemble median. For period #4 it was slightly higher.

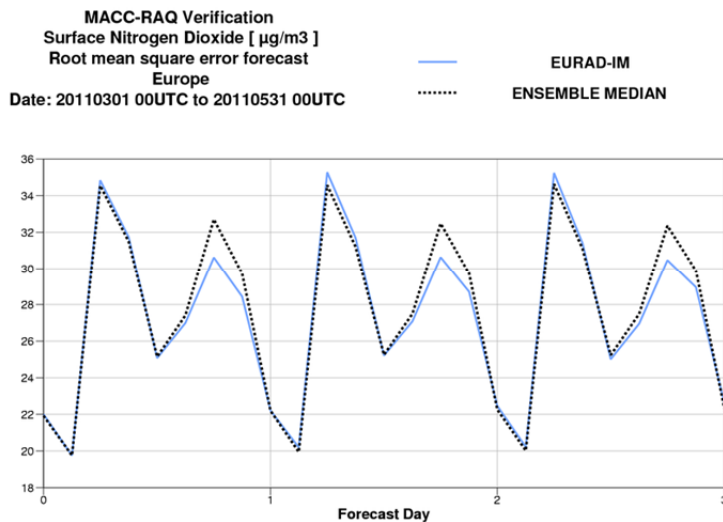


Compared to the ensemble median the correlation is lower at night and during forenoon. For period #4 the correlation was independent of time of day lower than that of the ensemble median.

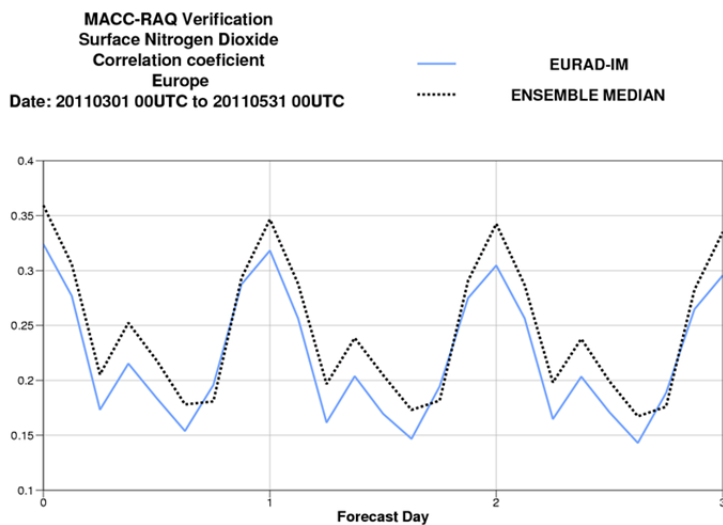
EURAD-IM: NO₂ skill scores, period #8 (March, April, May 2011)



The negative bias is partly due to an underestimation of nitrogen oxides at urban traffic sites, which are not representative for the current model resolution. The diurnal cycle of the bias is very similar to that of the ENSEMBLE product as it was also the case for period #4.

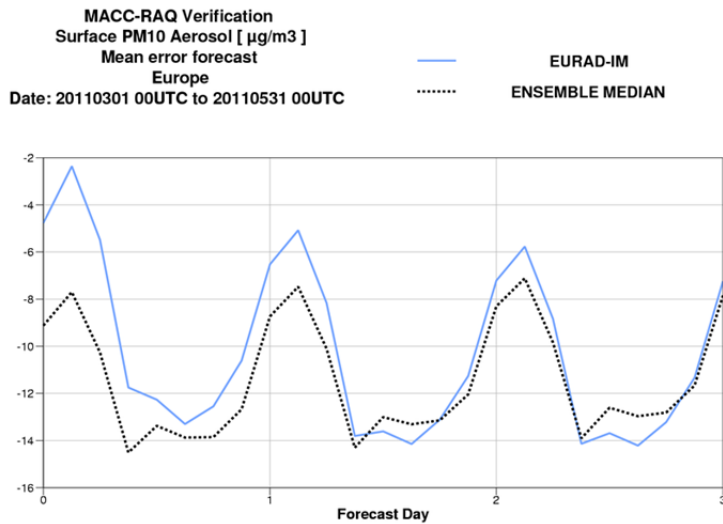


Magnitude and diurnal cycle of the root mean square error of Nitrogen Dioxide are very similar to period #4 and to that of the ENSEMBLE product.

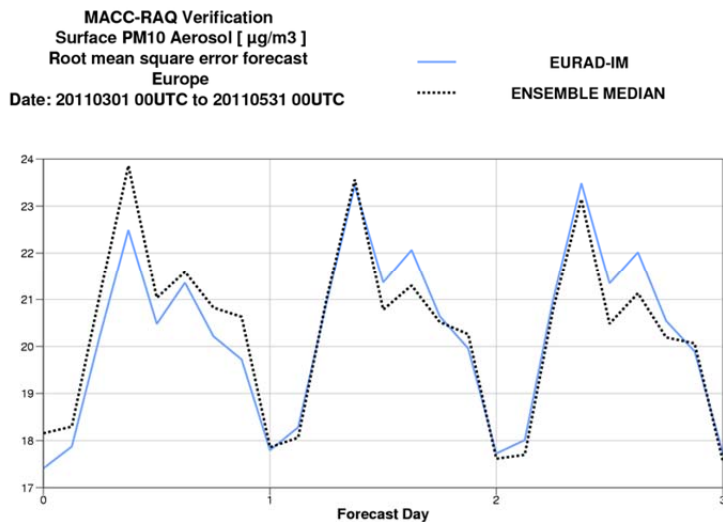


The variability of urban measurements can not well be represented with the current model resolution of 15 km. This is probably the cause of the low correlation coefficient, which is also not significantly higher for the ensemble median.

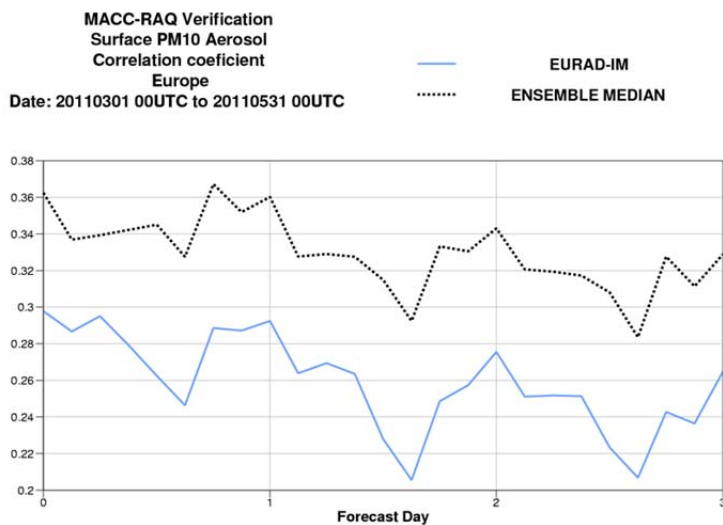
EURAD-IM: PM10 skill scores, period #8 (March, April, May 2011)



Under prediction of surface PM₁₀ concentrations is a common feature in air quality modelling, even for sophisticated models. Compared to the ENSEMBLE product the negative bias is especially for the first forecast day slightly lower. The relatively low bias during the first hours of the forecast is an implication of the initialization of the forecast with the air quality analysis for the previous day. In period #4 the PM₁₀ bias was during the whole 72h forecast slightly lower than that of the ensemble median.



Magnitude and diurnal cycle of the root mean square error are similar to that of the ENSEMBLE product. Again as consequence of forecast initialization with analysis results, compared to the ensemble median the rmse is slightly lower for the first forecast day. This feature was not visible in period #4.

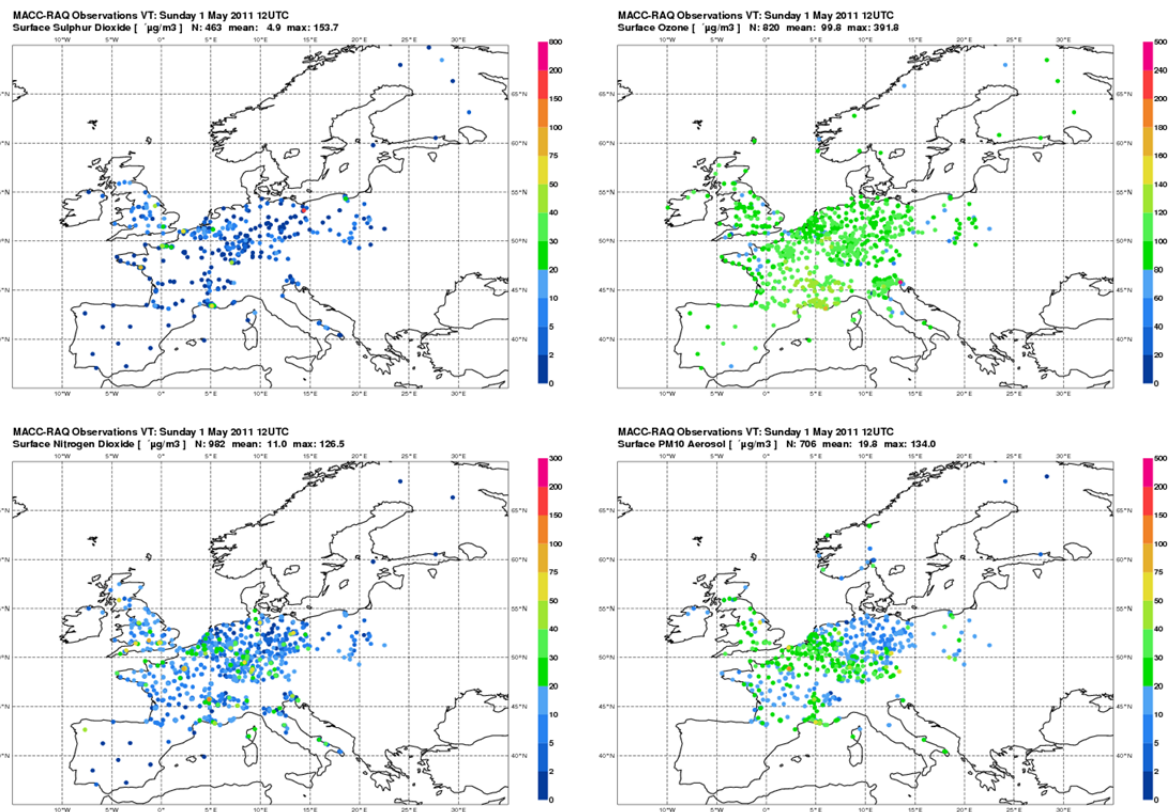


As for period #4 the correlation coefficient is lower than that of the ENSEMBLE product but its diurnal cycle is comparable. The reason for the degradation in model skill with forecast time is unobvious.

Verification report for quarter #9

This verification report covers the period June/July/August 2011. For this report, average skill scores (bias, root mean square error, correlation) for the EURAD-IM model are successively presented for three pollutants : ozone, NO₂ and PM10. The skill is shown for the entire forecast horizon 0 to 72h (3-hourly values), allowing to evaluate the entire diurnal cycle and the evolution of performance from day 1 to day 3.

For this verification period, as was the case on the MACC website, verifications are performed against all available data in Near-Real-Time (NRT) for the following countries: Belgium, Czech Republic, Denmark, Finland, France, Germany, Greece (Athens area only), Italy (not all regions), Netherlands, Norway, Poland, Spain, Sweden and the United Kingdom. The total number of sites is typically up to: 900 for ozone, 1200 for NO₂, 550 for SO₂, 300 for CO, 900 for PM10. As an example, the data coverage for Sunday May 1st 2011 12UTC is depicted below.

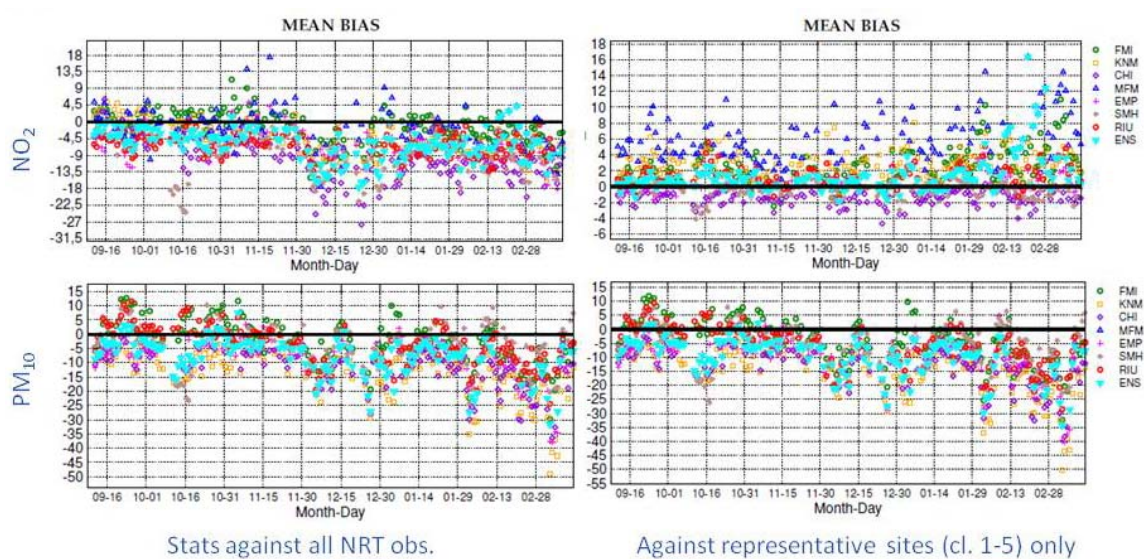


Near-Real-Time data coverage (May 1st 2011, 12 UTC)

Within MACC, the D-INSITU subproject is working with the European Environment Agency (EEA) to set up a new, more extensive and robust Near-Real-Time dataflow. An EEA European Air Quality data stream is available since the spring of 2011 and it has been checked by D-INSITU partners (in particular NILU) against the data currently received by MACC in NRT, which results from *ad hoc* bilateral agreement with Environment Agencies in

14 different countries. While there is an overlap between the two datasets, there is still a considerable number of differences. Briefly, the EEA dataset has more reporting sites for ozone and less for the other species. Also, there is a great interest in attempting to merge the two data sources, by helping for instance EEA to get access to data in the countries with which GEMS-MACC has been in contact and which do not provide all their NRT data to EEA. While this does not change the general objective to move to a EEA-based dataflow, it was felt that this evolution was not yet readily feasible for the last periods of MACC; this will be accomplished in MACC-II. A further advantage will be that data will arrive sooner, typically less than 3 hours after measurement. Currently, hourly data from the day before are available to MACC between 2 and 10 UT every day, depending on the country: this delays the possible start of daily verification calculations and makes it impossible to base the daily forecasts upon the analysis of the day before -as forecasts have to be delivered early enough every morning, in order to serve users' needs.

For the NRT verification of forecasts, the typology of sites is currently not taken into account: there is no uniform and reliable metadata currently for all regions and countries, which have all different approaches to this documentation. Skill scores are thus computed using all the data received. Within MACC, work has been carried out [Joly and Peuch, 2012] to build an objective classification of sites, based on the past measurements available in Airbase (EEA) ; see D_R-ENS_5.1 for more details. This classification can now be used in order to restrict verification only to the sites that have a sufficient spatial representativeness. Currently, about half of the sites used in the verification are declared "urban" in Airbase metadata and would be in principle not representative enough for comparing against forecast models that have horizontal resolutions of approximately 0.2°. However, our findings indicate that a significant fraction of sites labelled "urban" or "suburban" has actually little local character (as seen in past time series of measurements) and could be in fact more representative than what could be inferred from the metadata information. The figure below shows scores computed using all MACC data available in NRT and using only data for sites from classes 1-5 of our objective classification (the "background" fraction).



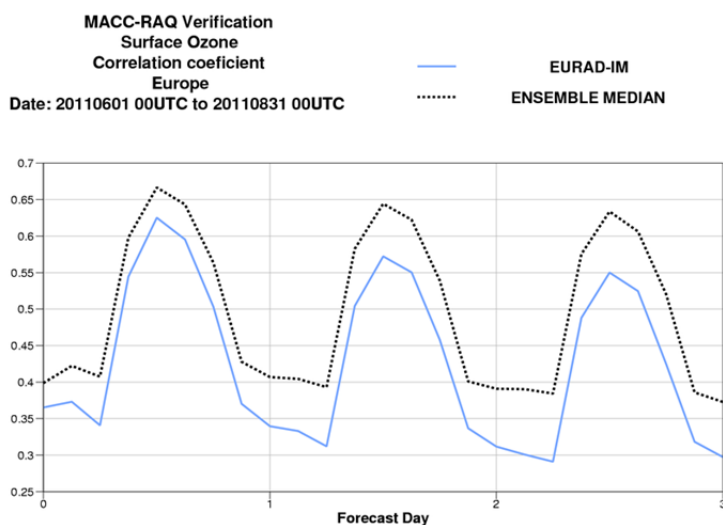
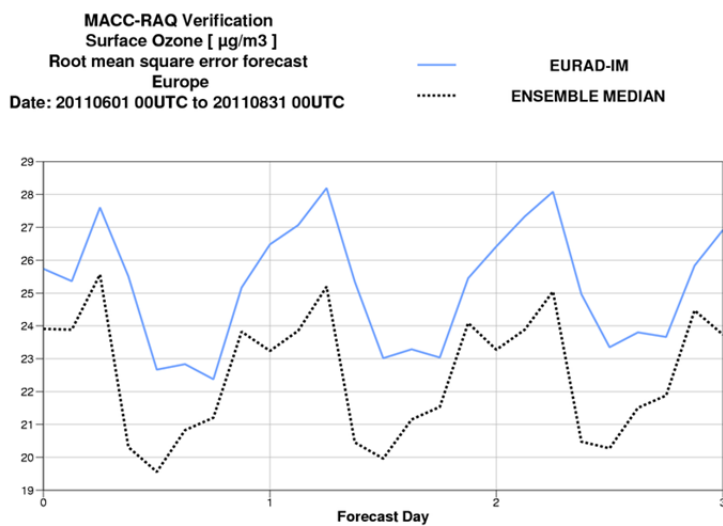
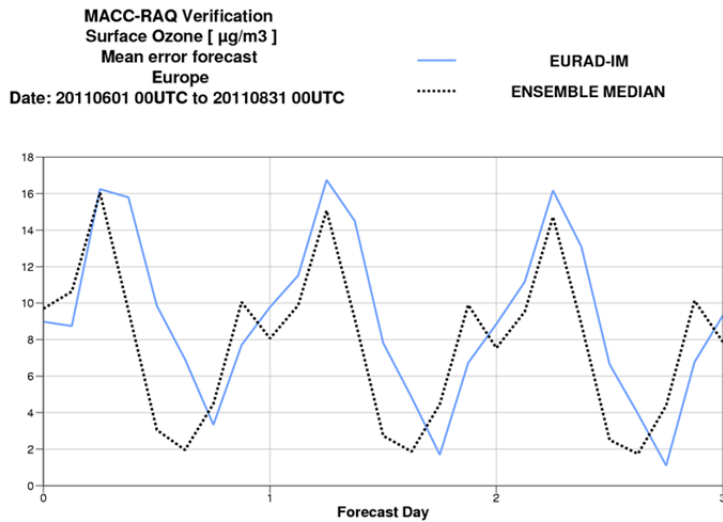
Sample model verification for the period 15/09/2010 to 28/02/2011 using all NRT sites (left) and using only most representative sites (classes 1-5) only (right). Values are for NO₂ (top) and PM₁₀ (bottom) for 0300 UTC.

While the statistical approach using only representative sites -according to the objective classification- is clearly the way forward (as it does not also thin too much the NRT data available), we see that overall skill scores are in general not too much affected by the observations from sites that have a local character, as illustrated here for PM10. Noticeable exceptions are winter night-time NO₂ values (top row on the figure), for which the general negative bias of the ensemble (around 5 µg.m⁻³) and of most of the individual models is entirely offset by using representative data only to compute skill scores.

As this evolution does not induce dramatic changes to our assessment, we have opted to finalise MACC using “all NRT data” statistics (to have continuity of approach during the project) and to switch to the “representative sites only” statistics only from the first quarter of MACC-II (DJF 2011-2012). This approach will also contribute to alleviate the issue of the large variation in site densities from one country to another: the countries with higher densities of observational sites, particularly Germany and France, will actually “lose” many more sites than the others (also in proportion). Yet, the issue remains that the overall skill scores presented here, and also on the MACC website in NRT, are largely governed by the behaviour of the models in the “data intensive” countries. In MACC-II, our verification procedures will be more segmented (by countries and by large continental regions: Northern Europe, Eastern Europe, Mediterranean...), which will allow to be increasingly more specific on the description of AQ products quality. At the same time, we acknowledge that the amount of information provided has to remain within reasonable bounds, in order not to confuse general users.

Joly, M. and V.-H. Peuch, 2012: Objective Classification of air quality monitoring sites over Europe, Atmos. Env., 47, 111-123.

EURAD-IM: ozone skill scores, period #9 (June, July, August 2011)

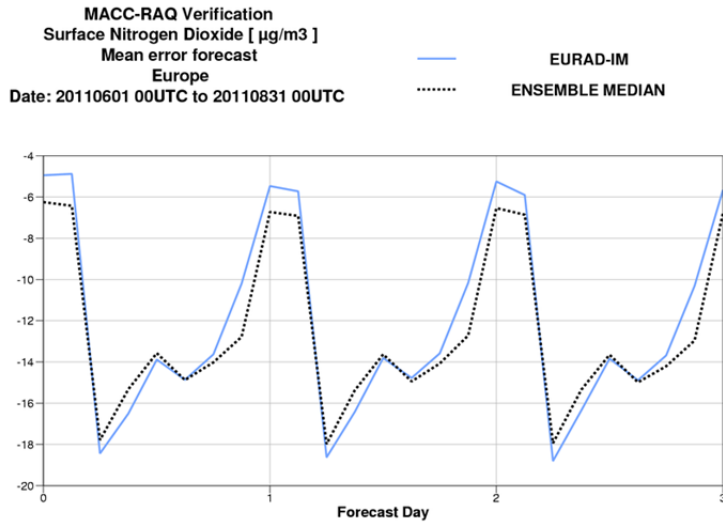


Compared to period #8 the positive bias of surface ozone is slightly increased but except of a phase shift similar to that of the ENSEMBLE product. Compared to period #5 (June, July, August 2010) the bias is lower probably due to improved modelling of photolysis frequencies during cloudy conditions.

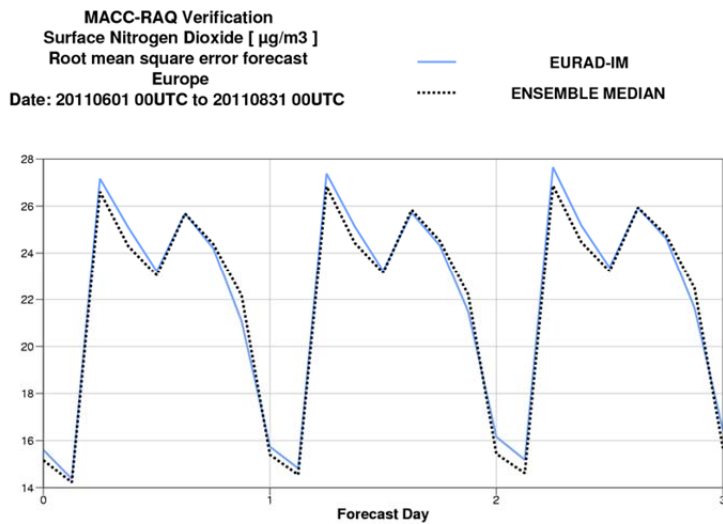
The root mean square error of the EURAD-IM Ozone forecast is significantly lower than for period #5 but still larger than that of the ensemble median.

The correlation coefficient is slightly lower than that of the ENSEMBLE product but significantly higher compared to period #5 and #8. The improvement with respect to period #5 and #8 is due to improved modelling of photolysis frequencies for cloudy conditions and a better performance of the EURAD-IM during summer.

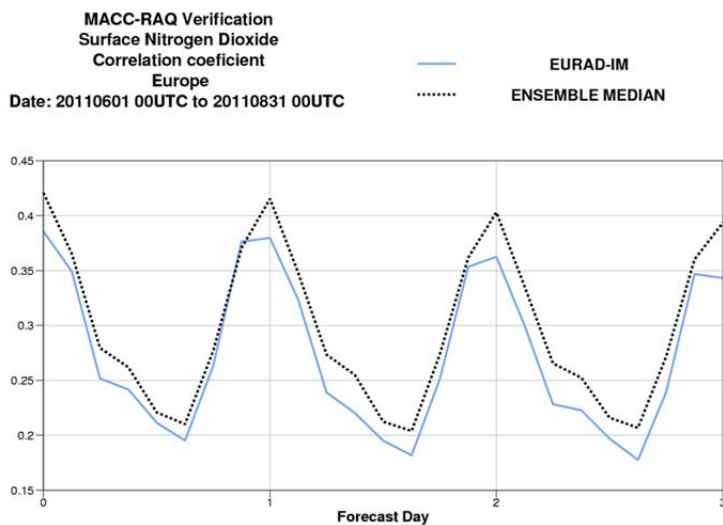
EURAD-IM: NO₂ skill scores, period #9 (June, July, August 2011)



The pattern of the mean forecast error of NO₂ is very similar as for the previous period and for period #5.

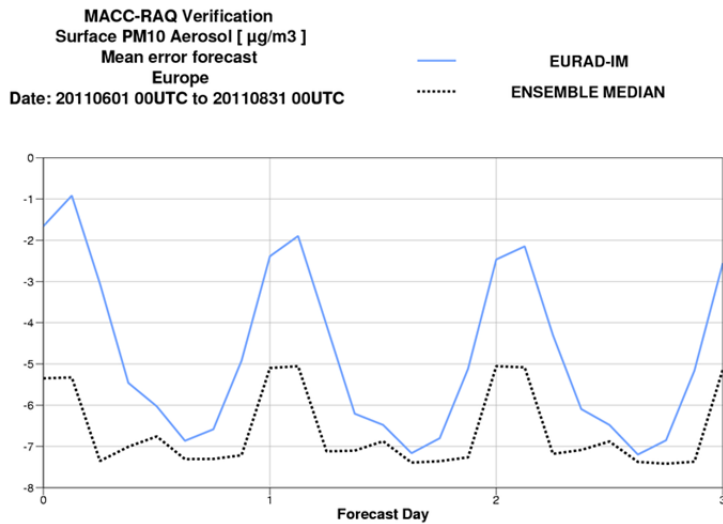


The root mean square error and its diurnal cycle are very similar to that of the ENSEMBLE product. Performance is better at night. The double peak is probably due to difficulties simulating rush hour conditions at poorly represented urban traffic sites. Compared to period #5 the rmse is slightly lower.

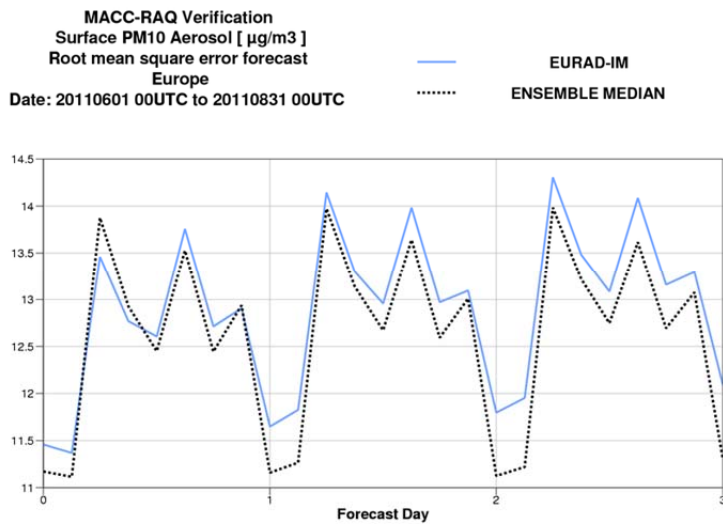


Compared to the ENSEMBLE product the correlation coefficient is slightly lower but higher than for period #5.

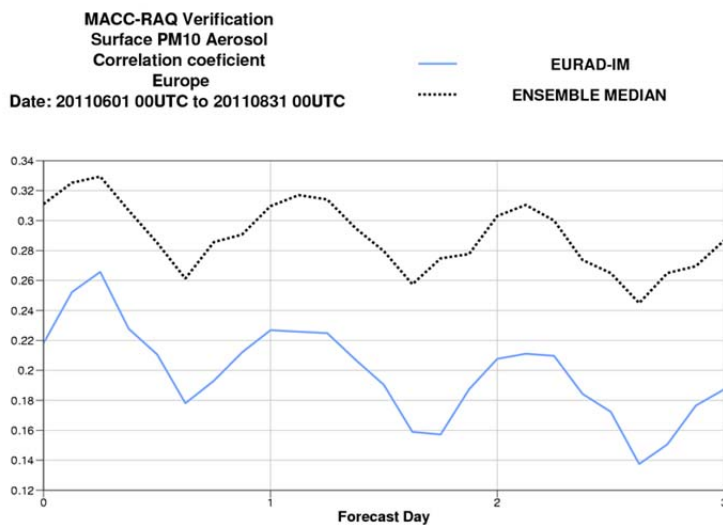
EURAD-IM: PM10 skill scores, period #9 (June, July, August 2011)



The mean bias of surface PM_{10} is lower than for period #8. The relatively low bias during the first hours of the forecast is an implication of the initialization of the forecast with the AQ analysis for the previous day. There are no significant differences compared to period #5.



Compared to period #8 the root mean square error decreases, probably largely due to the lower bias. The degradation in model skill with forecast time is not as obvious as for period #5. The triple peak is also visible in period #8 but lesser high in the morning.



The correlation coefficient is lower than that of the ENSEMBLE product but comparable to period #5.